1981

GAS DISPERSION NEAR A CUBICAL MODEL BUILDING
PART I: MEAN CONCENTRATION MEASUREMENTS

by

Wen-Whai Li and Robert N. Meroney

Fluid Mechanics and Wind Engineering Program
Department of Civil Engineering
Colorado State University
Fort Collins, Colorado 80523
U.S.A.

submitted to

Journal of Industrial Aerodynamics
and Wind Engineering

September 1981

CEP81-82WWL-RNM9a

GAS DISPERSION NEAR A CUBICAL MODEL BUILDING
PART I: MEAN CONCENTRATION MEASUREMENTS

Wen-Whai Li and Robert N. Meroney

Fluid Mechanics and Wind Engineering Program
Department of Civil Engineering
Colorado State University
Fort Collins, Colorado 80523
U.S.A.

Summary

The dispersion of effluent plumes emitted on or in the near wake region ($x/H \leq 5.0$) of a cubical model building have been examined. The model study was performed in a wind tunnel with a simulated neutral stratified shear layer. Mean concentration measurements were made on the model building for three different roof vent locations and three different building orientations. A full-scale measurement was conducted in the near wake region for central roof vent release.

The concentration level on the lee face of a model building is greatly reduced by the presence of a sharp edge of the model building. The optimum location for intake vent on the building, with equal vent exhaust to vent intake distance, is a position away from the downwind direction and at a location where it cannot "see" the exhaust vent. Orientation of the building at an angle of 45 degrees results in a secondary peak concentration on the building and in the near wake region.

Introduction

Mean concentration distributions of effluent plumes emitted on or near buildings is a common concern to health physicists, regulatory agencies, and air conditioning engineers. There is relatively little guidance available in handbook format, and the problem is difficult to

deal with theoretically. It is therefore an aspect of dispersion which is ideally suited for study in wind tunnels or water channels.

Halitsky (1) conducted his verification experiments of the surface concentration on a model building under conditions of non-turbulent, uniform, mean velocity profile and isothermal temperature. The data may be distorted, as discussed by Wilson (2) and Meroney (3), since Halitsky failed to simulate the random fluctuations of atmospheric turbulence and the relative length scale. Wilson presented a measurement on the building surface for various vent locations and building sizes in a simulated atmospheric boundary layer. A value of $B = 0.11$ was suggested by Wilson for the minimum dilution factor of roof vent releases. The tests performed by Wilson and Halitsky were with the upwind face perpendicular to the wind. However, the effects of other building orientations to the wind have not been reported. Hence the purpose of the mean concentration measurements on the building in this study is to stipulate the building concentration distributions which result from different roof vent locations and building orientations for a simple building geometry.

The behavior of mean concentration distribution in the wake of a building has been provided by several authors, (Huber (4)). But most measurements were concentrated in the region beyond the building cavity zone. Therefore the other purpose of this study is to specify the concentration level and distributions which occur in the near wake region behind a cubical model building.

The associated concentration fluctuation measurements are reported in the second part of this study. The purpose is to provide a better understanding of the concentration behavior in a model building wake.

In the study of mean concentration behavior the general non-dimensional concentration coefficient, K, is defined as the ratio of the actual concentration, χ, at any point in the field to a reference concentration:

$$K = \frac{\chi L^2 V}{Q}$$

where L = reference length, V =reference velocity and Q = contaminant release rate.

In the present study, L and V are chosen as $\sqrt{A_c}$ and U_H, respectively, where A_c is the cross wind, cross-sectional area of the building for $\theta = 0°$ orientation and U_H is the velocity at the height of the building. Since the projected frontal area will be proportional to A_c it is felt that A_c is a more convenient variable.

All the model tests in this paper were made with a passive source (little or no effluent momentum) located in the building surface. This configuration would be representative of a leak in a nuclear reactor containment structure or the discharge from a small flush vent, but it would not be representative of a large diameter, higher velocity jet release common in modern ventilation systems. Concentrations in passive vent plumes decay more rapidly than in jet plumes because the latter have an initial undiluted core. Therefore a minimum dilution criterion developed for passive releases may not be sufficiently conservative for jet releases if there is reason to believe that the intake will be exposed to plume centerline concentrations.

Experimental Facilities and Measurements

Mean concentration measurements and the system imposed error are presented followed by a brief description of the wind tunnel facility and the boundary layer parameters in this section.

Wind Tunnel Facility and the Boundary Layer

The facility used was the thermally stratified wind tunnel of the Fluid Dynamics and Diffusion Laboratory at Colorado State University. The tunnel was designed for simulation of a thermally stratified boundary layer in the atmosphere; however, the boundary layer simulated was neutral for this study. The boundary layer used in the study was developed over the length of the test section (240 cm downwind from the entrance). Spires, barriers and a distributed surface roughness were utilized to provide a fully developed boundary layer approximately 30 cm deep with a power law exponent 0.19 throughout the test section. Figure 1 shows the mean velocity and local turbulence intensity profiles as a function of non-dimensional height in the boundary layer. The height in the plot is normalized with respect to the boundary layer thickness. The local turbulence intensity is defined as the ratio of the root-mean-square velocity, $\sqrt{u^2}$, to the mean velocity, U, at a given height in the boundary layer. The effective roughness height, Z_o, was 7.5×10^{-3} cm and the integral time scale, $\tau = \int_o^\infty R_u(t)\, dt$, was found to be 0.25 sec at $Z/H = 0.3$, and $U_H = 330$ cm/sec. Table 1 shows some characteristic parameters of the simulated atmospheric boundary layer. Additional data concerning the wind tunnel facility and the boundary layer are described by Li, et al. (5).

Mean Concentration Measurements

Given a desired wind tunnel modeled flow configuration, pure helium was released at a flow rate of 12.5 cm^3/sec (exit velocity ratio, $U_e/U_H = 0.19$). Diffusion patterns were allowed to stabilize three minutes before any concentration measurement was taken. The concentration of the tracer gas (helium) was withdrawn by a sampling probe and

analyzed by a thermal conductivity gas chromotograph (TCGC). The sampling probe (1.47 mm O.D. and 1.06 mm I.D.) was made of a hypodermic, stainless steel tube. The probe was mounted on a traversing mechanism and perpendicular positioned with a distance, 0.3 mm, off the surface of the model building for surface concentration measurements. The TCGC was modified so that continuous sample analysis was possible. Background concentrations were examined before and after each measurement to correct for drift.

A plexiglas model (5 cm x 5 cm x 5 cm) was constructed to simulate a cubical building in the wind tunnel. The degree of blockage was less than 1 percent of the tunnel cross sectional area.

The dimensionless concentration coefficient, $k_e = \chi_e AU/Q_e$, is equal to 660 in the present study. The exit momentum effect is neglected since $(\rho_e/\rho_a)^{0.5}\ U_e/U_H$ is only equal to 0.07.

Data Reduction

The bridge output of the TCGC was monitored by a voltage meter and recorded by a X-Y recorder. A calibration curve between the voltage outputs and the actual mean concentrations was obtained by running the calibration gases through the TCGC. An interpolation scheme developed from quasi-Hermite piecewise-polynomials based on local procedures suggested by Akima (6) was employed to interpolate data for contour plot generation.

The total system error of the measurement is imposed by the instrument sensitivity (~30 ppm), the background concentraion of helium in the air within the wind tunnel (<30 ppm), and the nonisokinetic nature of the sampling near the surface (~10 percent). The resultant uncertainty in the concentration data is below 20 percent.

Results and Discussion

The results and discussion presented in this section are divided into five categories. Concentration measurements on a model building and in the building wake are presented for three wind directions. Analysis of minimum dilution factor is made for surface concentration measurements.

Concentration Measurements on the Model Building Normal to the Wind

Figure 2 through Figure 10 show the isopleth graphs of constant concentration coefficient K. Each K isopleth formed a closed contour originating from the vent location unless intercepted by the presence of the ground. These contours display a degree of distortion or displacement depending on vent location and wind direction. Isopleth lines tend to retain a closed shape though they are distored into irregular lobes.

The concentration level on the cubical building for different roof vent emission locations and wind normal to the frontal surface are displayed in Figure 2 to Figure 4. It was found that the concentration level on the building decreased as it passed around a sharp edge on the building. The effect of the sharp edge imposed on the surface concentration level is shown in Figure 11, where concentration coefficient is plotted versus distance from the vent location. A rapid rate of decrease is found in Figure 12 just after the gas passed over the edge point (edge points are indicated on the figure). The effect of the sharp edge is predictable, since the gas plume passing the sharp edge continued to follow a trajectory similar to the flow pattern around the building. Thus an "extra distance" was traveled by the gas plume after it left the edge and before it entered the region of the lee face. Moreover, the dispersion process in the near wake tends to reduce the

concentration of the reattached gas plume. Therefore, for an intake point which cannot "see" the vent location one observes lower concentration than an intake point, with equal distance from the exhaust vent, which can "see" the vent location. The concentration level at points which can "see" the vent location in the near wake region for $\theta = 0°$, central roof vent release are also shown in Figure 12. By considering those points which can and cannot "see" the vent but with equal distance from the vent location, the effect of the sharp edges effect become obvious. The sharp edge effect was found most significant within the region 1/6 H from the edge on the lee face. The plume appeared to reattach on the lee face of the building at a height 5/6 H from the ground level. The sharp edge effect was not as significant for the side building face, since the flow tends to advect the gas plume in the downwind direction.

Concentration Measurements on the Model Building Skewed to the Wind

Figure 5 to Figure 7 show isopleths for buildings rotated 45 degrees to the wind direction. A secondary peak occurring near the edge of the building was found and is shown in Figure 5a. This phenomenon is significant for $\theta = 22.5°$ and $\theta = 45°$ orientation (as shown in Figures 5a, 6a, 7a and 10a). A recirculation flow occurred in the separation zone which advected the contaminants upwind across the top edge from the sides. Two counter-rotating vortices are induced at the upstream roof edges when the wind direction is changed from the normal position. The two vortices tend to return the contaminants to the roof. The interaction between the recirculation flow and the vortice produces a secondary peak of concentration on the roof near the downstream edge.

Dilution Factors

Surface concentration data in the form of dilution factors, $D = K_e/K$, were plotted against the non-dimensional distance $r/\sqrt{A_c}$ from the exhaust vent location, as shown in Figure 13 through Figure 15. The minimum dilution factor, $D_{min} = BK_e(r/\sqrt{A_c})^2$, corresponds to maximum surface concentration which is expected at a given distance from a roof vent. Previous expressions proposed by different authors for minimum dilution factors are also noted on the figures. For the $\theta = 0°$ case a value of $B = 0.11$ (suggested by Wilson (2)) provides a linear limit beneath all measurements. Some recent measurements around two nuclear facilities were also examined by Meroney (3). Again $B = 0.11$ provides a lower bound for 99 percent of all measurements. Figure 13 indicates that the data for $\theta = 0°$ case agree well with the prediction. Figure 15 shows that $B = 0.11$ may not be a safe lower bound for buildings at large angles of orientation to the approach flow. $B = 0.11$ does appear satisfactory for the $\theta = 22.5°$ cases; however, a limited number of the data for $\theta = 45°$ fall below the $B = 0.11$ line. These data were measured in the region where three building edges intersected. At similar distances from the vent location concentrations obtained for the $\theta = 45°$ case are higher than concentrations observed for the $\theta = 0°$ case by a factor ranging from 3 to 9. A comparison of data for equal distances from the vent location for $\theta = 22.5°$ and $\theta = 0°$ suggest a similar tendency with a factor ranging from 2 to 5 (as shown in Figure 11). Therefore, a correction factor is recommended to adjust for an orientation effect upon minimum dilution factor.

$$f(\theta) = \frac{1}{1 + \frac{4\theta}{\pi}} \quad , \quad 0 \leqq \theta \leqq \frac{\pi}{4} \quad , \quad \text{where } \theta \text{ is in radions}$$

Concentration Measurements in the Near Wake Region Behind a Model Building Normal to the Wind

Isopleths of constant K for $\theta = 0°$ and a central roof vent release have been plotted on the x-y plane for different x/H sections (as shown in Figure 16). Isopleths for the centerline longitudinal section is displayed in Figure 17. The maximum value of the concentration level in the crosswind plane occurred on the ground after $x/H = 7.0$. Figure 18 indicates that the centerline ground concentration increased from the building edge to a maximum, then it gradually decreased with $x/H = 4.0$ for $\theta = 0°$ case and at $x/H = 2.5$ for $\theta = 45°$ case.

The vertical mean concentration profiles at $y = 0.0$ for $\theta = 0°$ and a downwind roof vent release are presented in Figure 19a. The downwash effect tended to entrain the effluents into the near wake region and to carry the effluents toward the ground for the downwind roof vent. Higher concentrations were observed closer to the ground than when compared with the central roof vent release. The maximum value of the crosswind concentration distribution for the downwind roof vent release occurred on the ground at $x/H = 5.0$, whereas the maximum value occurred at $x/H = 7.0$ for the central roof vent release.

Concentration Measurements in the Near Wake Region Behind a Model Building Skewed to the Wind

Vertical mean concentration profiles at $y = 0$ for $\theta = 45°$ top center roof vent release are displayed in Figure 19b. The downwash effect due to a change in the wind direction becomes more significant than for the case of $\theta = 0°$. The maximum value of the crosswind concentration distribution for $\theta = 45°$ and top center release occurred on the ground when x/H exceeds 2.5. The crosswind ground level

concentration profile is shown in Figure 20. Two secondary peaks occurred near the edges of the plume. The two peaks are due to the two counter rotating vortices, which are generated by the orientation of the building. The vortices originate from the upstream edges of the roof and travel along the wind direction passing by the edge of the near wake region.

Conclusion

Measurements of gaseous dispersion have been made on a cubical model building in a neutral stratified shear layer and in the near wake region ($x/H \leq 5$) behind a model building for roof vent emissions. Based on the experimental results obtained in this study and a comparison with similar experiments by others, the following observations can be made.

1. Concentration isopleths on a building surface will appear as closed continuous curves with their centers at the vent location unless intercepted by the presence of the ground. These isopleth shapes may be expanded (compressed) or distorted depending on the flow conditions or building configuration.

2. With equal vent exhaust to vent intake distance the mean concentrations decrease as the intake directions deviate from the wind direction. The concentration level on the lee face of a model building is greatly reduced by the presence of a building corner. The effect of the edge becomes insignificant if the intake direction deviates from the direction of the main gas plume. Therefore for different roof vent locations and different wind orientations, given equal vent exhaust to vent intake distance, the optimum location for intake vents is a position away from the downwind direction and at a location where it cannot "see" the exhaust vent.

3. The algorithm proposed for calculation of minimum dilution on a building, $D_{min} = BK_e(r/\sqrt{A_c})^2$ and $B = 0.11$ given by Wilson (1976) is supported by these measurments for the $\theta = 0°$ orientation. The value, $B = 0.11$, provides a lower bound for more than 99 percent of the measured data. Orientation of a building such that wind does not approach normal to a building face tends to decrease minimum dilutions. A correction factor depending on orientation angle was found to adjust prediction algorithms where

$$f(\theta) = \frac{1}{1 + \frac{4\theta}{\pi}} \quad 0 \leqq \theta \leqq \frac{\pi}{4} \quad \text{and} \quad D_{min} = Bf(\theta)\, K_e \left(\frac{r}{\sqrt{A_c}}\right)^2$$

4. Orientation of the building at an angle of 45° results in a secondary peak concentration on the crosswind, ground concentration distribution. This secondary peak occurs at the edge of the near wake and near the ground.

5. Orientation of a building a angles other than normal to the wind tends to increase the concentration level as a result of an enhanced downwash effect in the near wake region. The maximum ground concentration in the near wake was found to occur at $x/H = 2.5$ for an $\theta = 45°$ orientation.

Acknowledgments

This research was conducted under contract No. AT(49-24)-0366 with the United States Nuclear Regulatory Commission, Office of Nuclear Regulatory Reserach. Financial support received is gratefully acknowledged. The authors also thank Dr. Robert Abbey, Jr., NRC and Dr. Jon A. Peterka, CSU, for their helpful suggestions and encouragement during the course of the research.

References

1. J. Halitsky, Gas Diffusion Near Buildings, ASHRAE Trans., Vol. 69, 1963, pp. 464-485.

2. D. J. Wilson, Dilution of Exhaust Gases from Building Surface Vents, ASHRAE Trans., Vol. 83, pp. 168-176.

3. R. N. Meroney, Turbulent Diffusion Near Buildings, Engineering Meteorology, E. Plate, editor, Colorado State University, CEP78-79RNM23. (1982).

4. A. H. Huber, Determination of Good Engineering Practice Stack Height, presented at the 70th Annual Meeting of the APCA, 1978.

5. W. W. Li, R. N. Meroney and J. A. Peterka, "Wind Tunnel Study of Gas Dispersion Near a Cubical Model Building, CER81-82WWL-RNM-JAP8, Colorado State University, 1981.

6. H. Akima, A New Method of Interpolation and Smooth Curve Fitting Based on Local Procedures, J. of the Assoc. for Computing Machinery, Vol. 17, 1970, pp. 589-602.

7. J. Counihan, Adiabatic Atmospheric Boundary Layer: A Review and Analysis of Data from the Period 1880-1972, Atmos. Environment, Vol. 19, 1975, pp. 871-905.

8. G. A. Briggs, Diffusion Estimation for Small Emissions, Atmospheric Turbulence and Diffusion Laboratory Report No. 79, NOAA, Oak Ridge, Tennessee, 1973, 61 p.

9. R. S. Scorer, Air Pollution, Pergamon Press, New York, 1968.

10. D. J. Hall, The Discharge of Fume Cupboard Effluents into the Atmosphere, LR845(AP), Warren Spring Laboratory, Dept. of Industry, Heitfordshire, SGI2BX, 1980.

11. R. N. Meroney and B. T. Yang, Wind Tunnel Study on Gaseous Mixing due to Various Stack Heights and Injection Rates above an Isolated Structure. No. C00-2053-6, U.S. Atomic Energy Commission Report, 1971.

12. R. S. Thompson and D. J. Lombardi, Dispersion of Roof-Top Emissions from Isolated Buildings, EPA-600/4-77-006, U.S. Environmental Protection Agency, 1977.

13. A. G. Robins and I. P. Castro, A Wind-Tunnel Investigation of Plume Dispersion in the Vicinity of a Surface Mounted Cube--II The Concentration Field, Atmos. Environment, Vol. II, 1977, pp. 299-311.

14. D. J. Koga and J. L. Way, Effects of Stack Height and Position on Pollutant Dispersion on Building Wake, Proceedings of the Fifth International Conference on Wind Engineering, 1979, pp. 1003-1018.

Nomenclature

A_c	Reference building area
B	Constant for minimum dilution factor
D	Dilution factor
H	Height of building
K	Non-dimensional concentration coefficient
K_e	Concentration coefficient at effluent vent
L	Reference length of building
Q	Contaminant release rate
$R_u(t)$	Autocorrelation function
U_H	Velocity at building height
U_e	Velocity of effluent
u'	Fluctuating velocity component
V	Reference velocity
χ	Observed concentration
θ	Building orientation
x,y,z	Coordinates, origin is ground level under the center of the roof
U_∞	Free stream velocity
δ	Boundary layer thickness

Table 1. Characteristic Parmaeters of the Simulated Atmospheric Boundary Layer

	Model Scale (1/2000)	Prototype	Field Result Counihan (1977)*
n	0.19	0.19	0.17
δ (m)	0.30	600	600
z_o (m)	7.5×10^{-5}	0.15	0.15
$\Lambda_{at}\ \frac{z}{\delta} = \frac{1}{20}$	0.0667	134	148
$\left(\frac{\sqrt{\overline{u'^2}}}{U}\right)\ \frac{z}{\delta} = \frac{1}{20}$	0.152	0.152	0.188
$\left(\frac{\sqrt{\overline{u'^2}}}{U}\right)\ \frac{z}{\delta} = \frac{1}{6}$	0.118	0.118	0.153
$\left(\frac{u_*}{U_\infty}\right)^2$	2.44 x 10-3	2.44×10^{-3}	2.26×10^{-3}
U_H = (m/sec)	3.3	--	--
Re_H	11050	--	--

*$n = 0.096 \log_{10} z_o + 0.016(\log_{10} z_o)^2 + 0.24$

$$\Lambda_{at}\ \frac{z}{\delta} = \frac{1}{20} = 108\ \frac{1}{z_o}^{1/6}$$

$$\left(\frac{\sqrt{\overline{u'^2}}}{U}\right) = 0.4 \times 2.49 \times (\log\ \frac{z}{z_o})^{-1}$$

$$\left(\frac{u_*}{U_\infty}\right)^2 = 2.75 \times 10^{-3} + 6 \times 10\text{-}4\ \log_{10} z_o$$

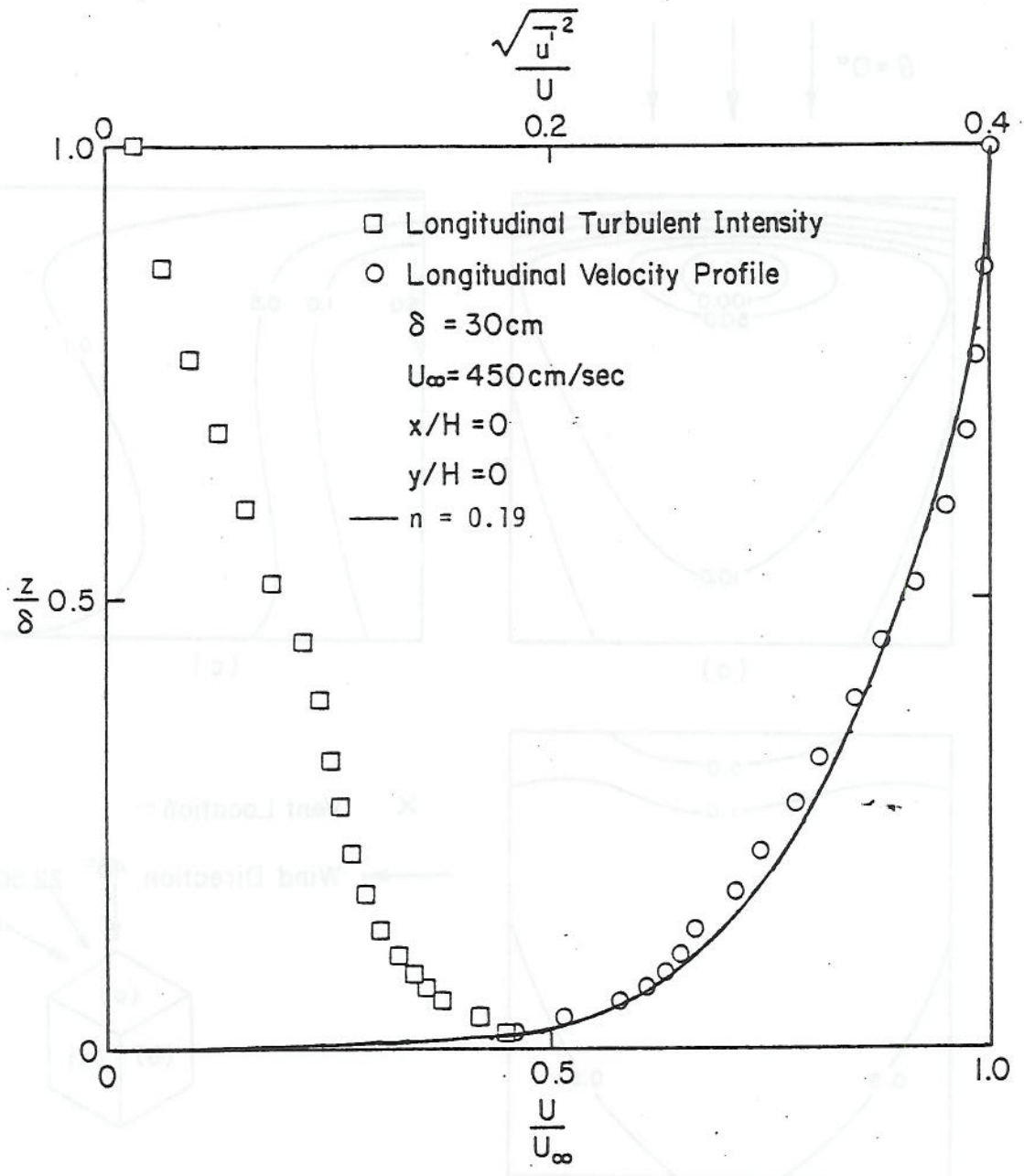

Figure 1. Mean velocity and turbulent intensity profile.

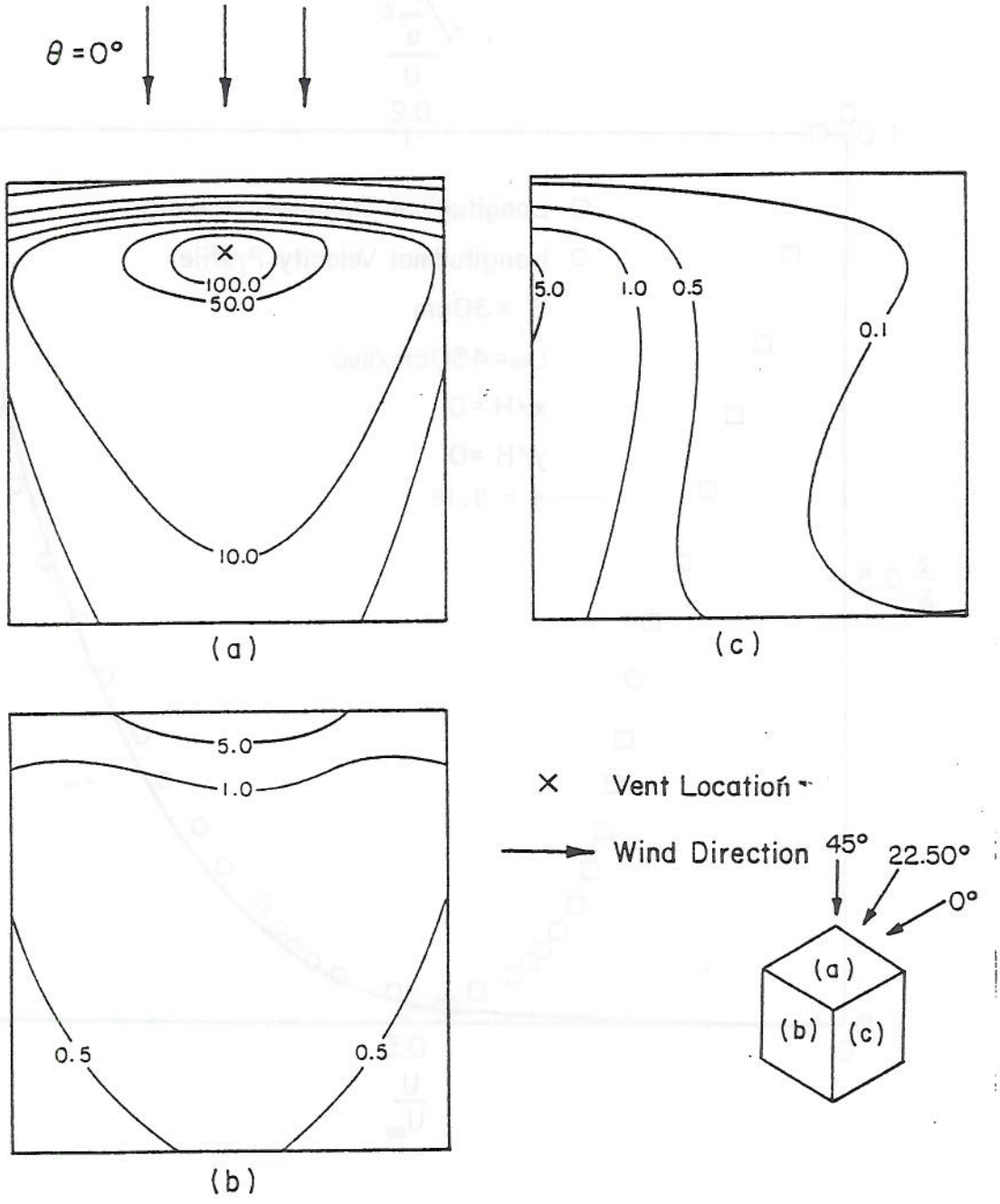

Figure 2. Concentration coefficient isopleths on a cubical model building (θ = 0°, upwind roof vent release).

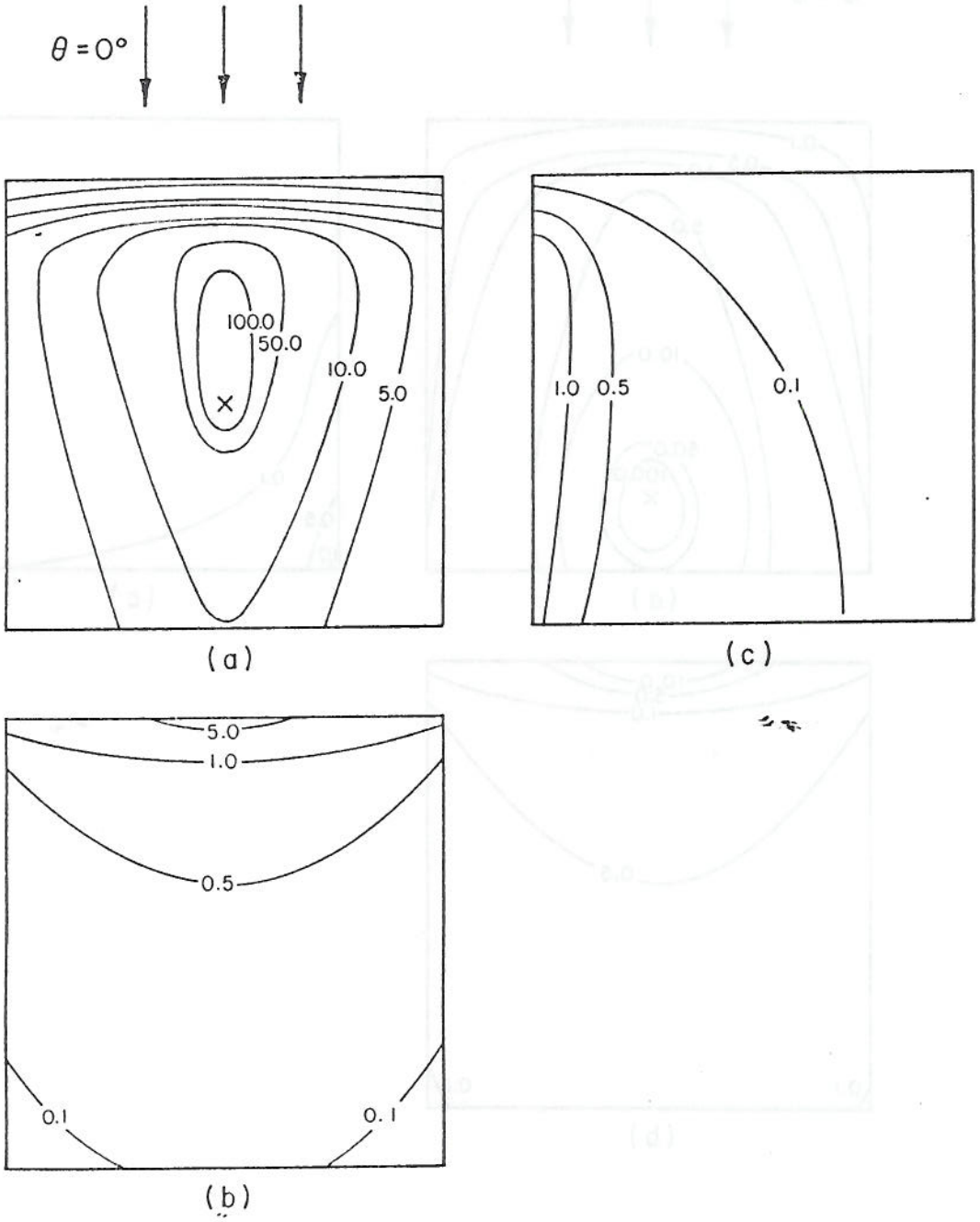

Figure 3. Concentration coefficient isopleths on a cubical model building (θ = 0°, central roof vent release).

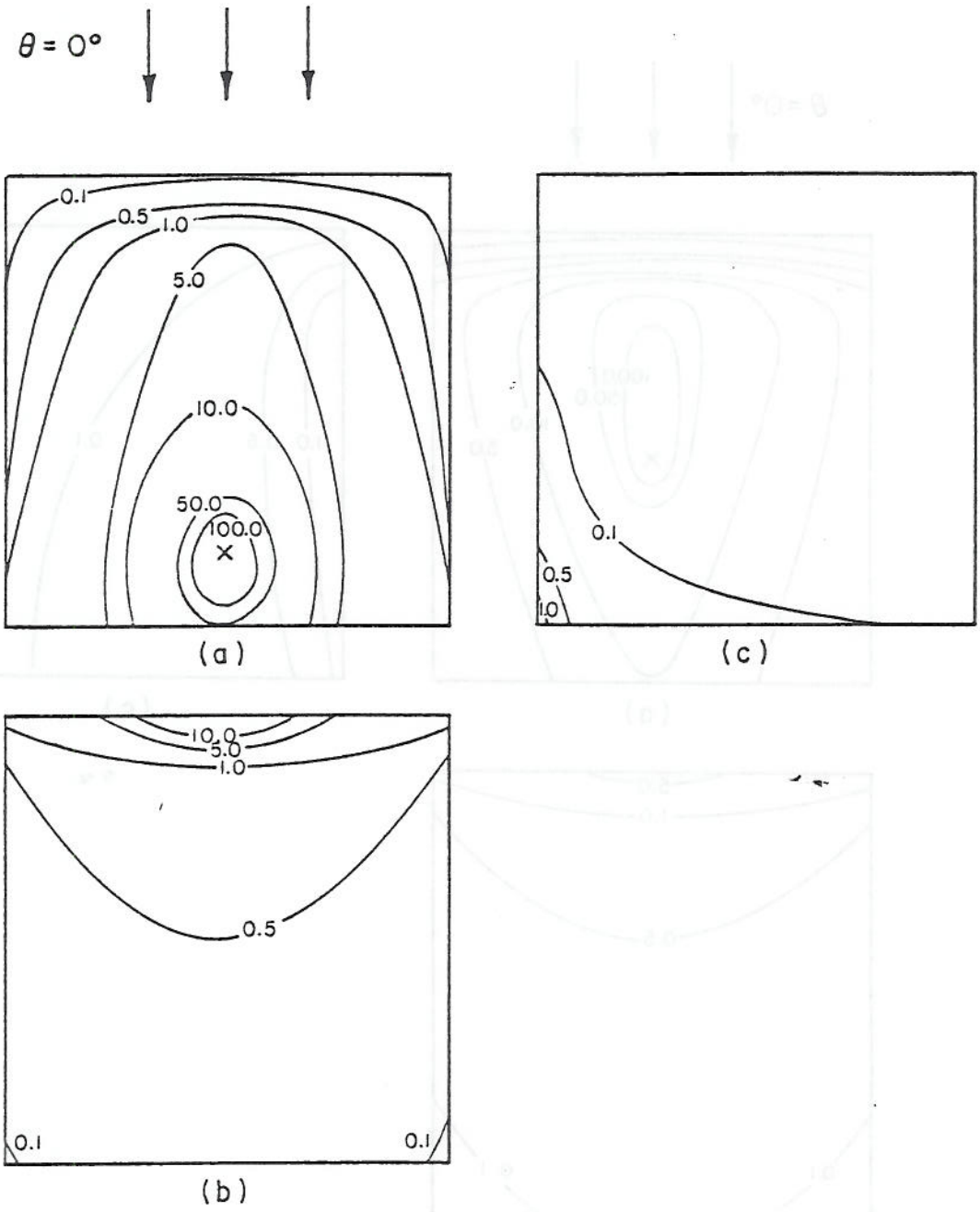

Figure 4. Concentration coefficient isopleths on a cubical model building (θ = 0°, downwind roof vent release).

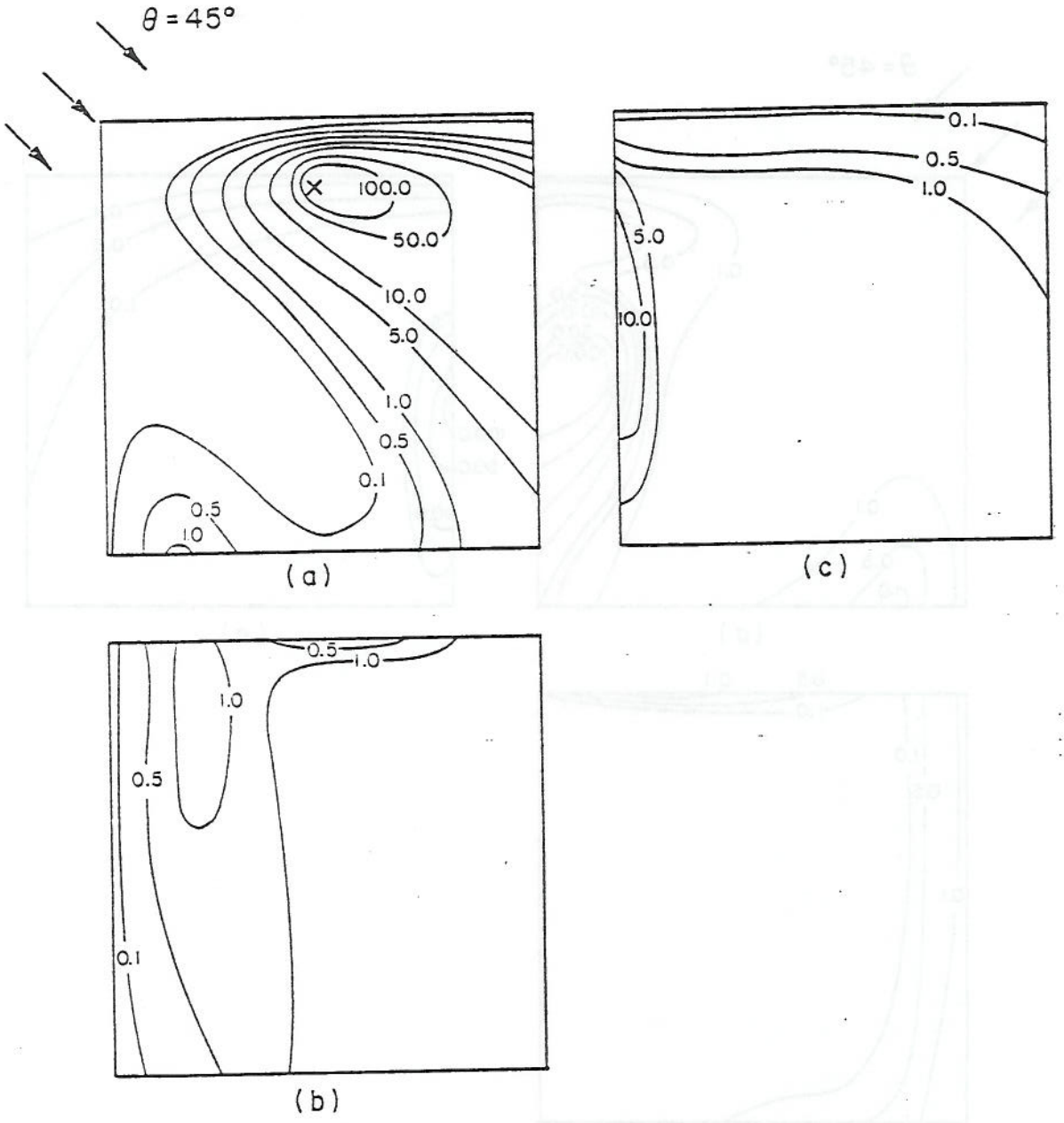

Figure 5. Concentration coefficient isopleths, K, on a cubical model building (θ = 45°, upwind roof vent release).

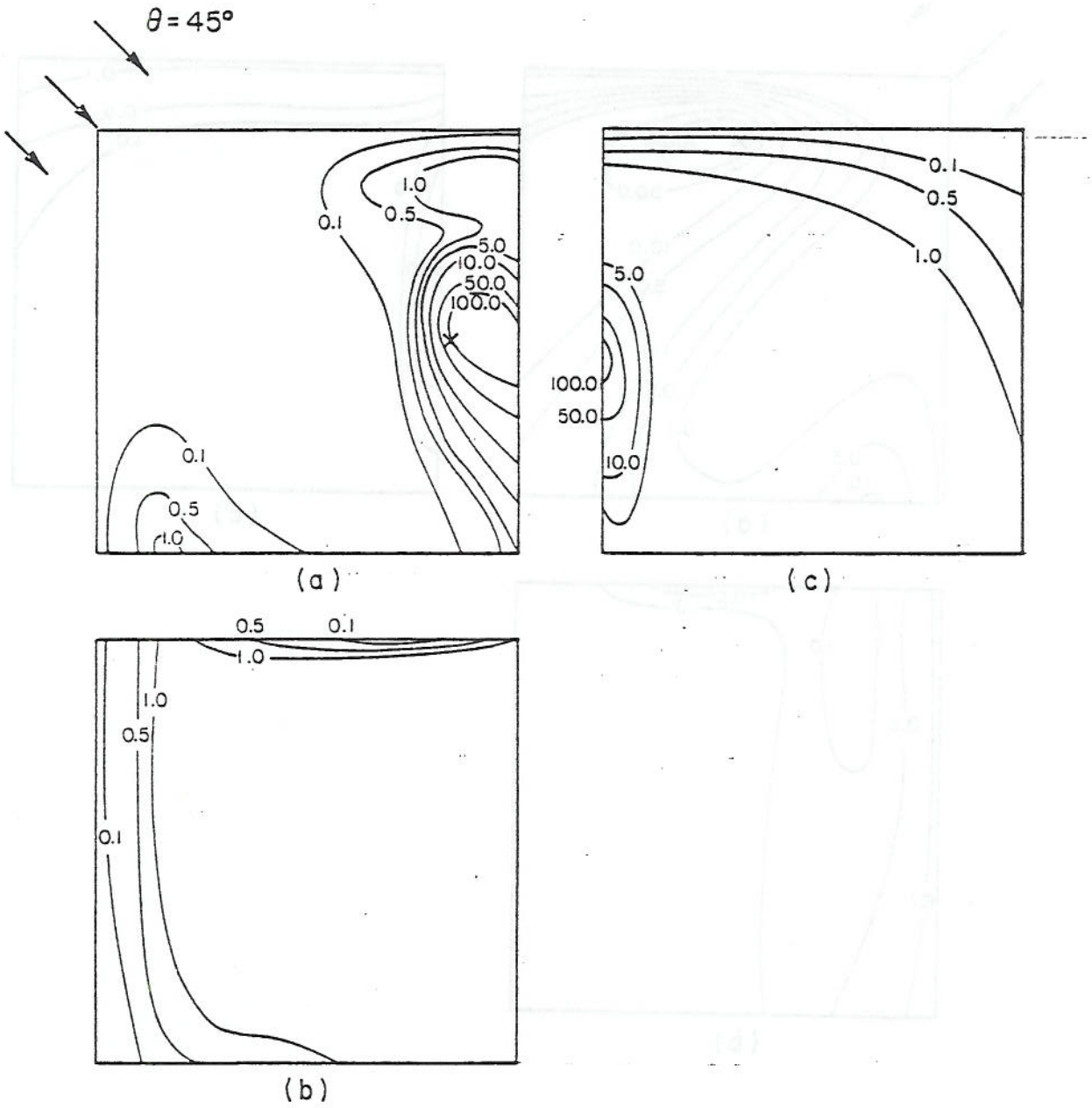

Figure 7. Concentration coefficient isopleths on a cubical model building (θ = 45°, downwind roof vent release).

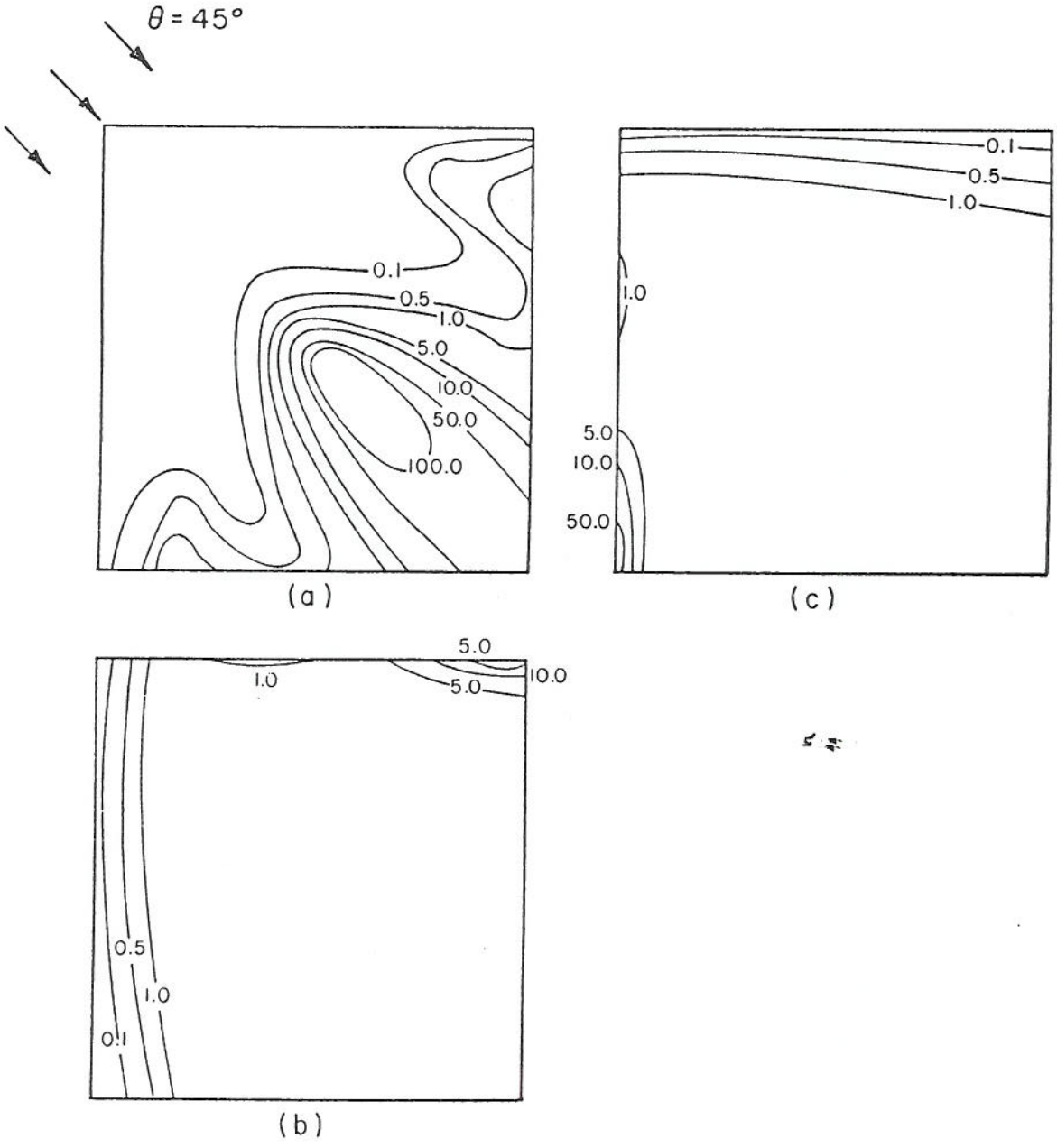

Figure 6. Concentration coefficient isopleths on a cubical model building (θ = 45°, central roof vent release).

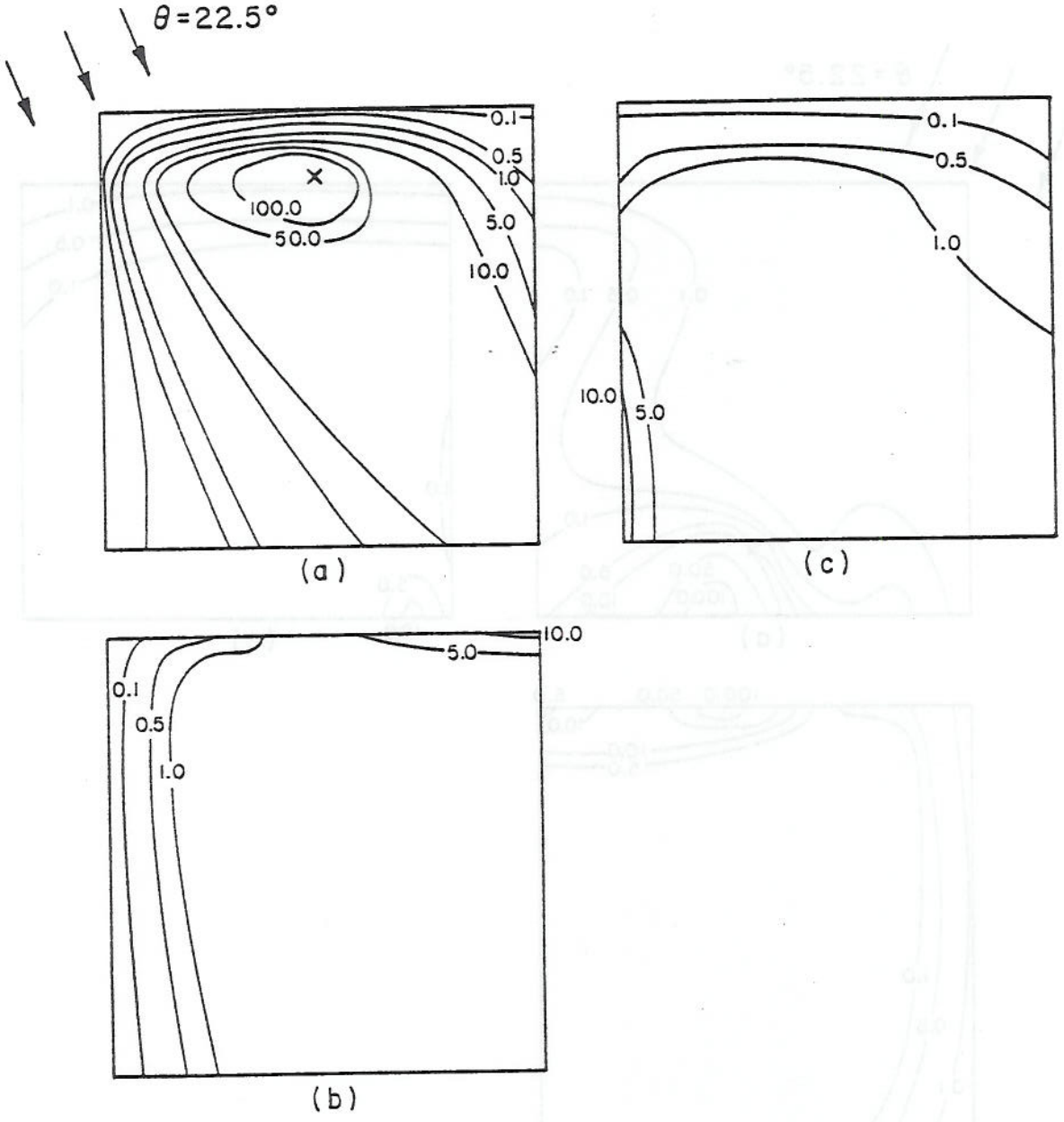

Figure 8. Concentration coefficient isopleths on a cubical model building (θ = 22.5°, upwind roof vent release).

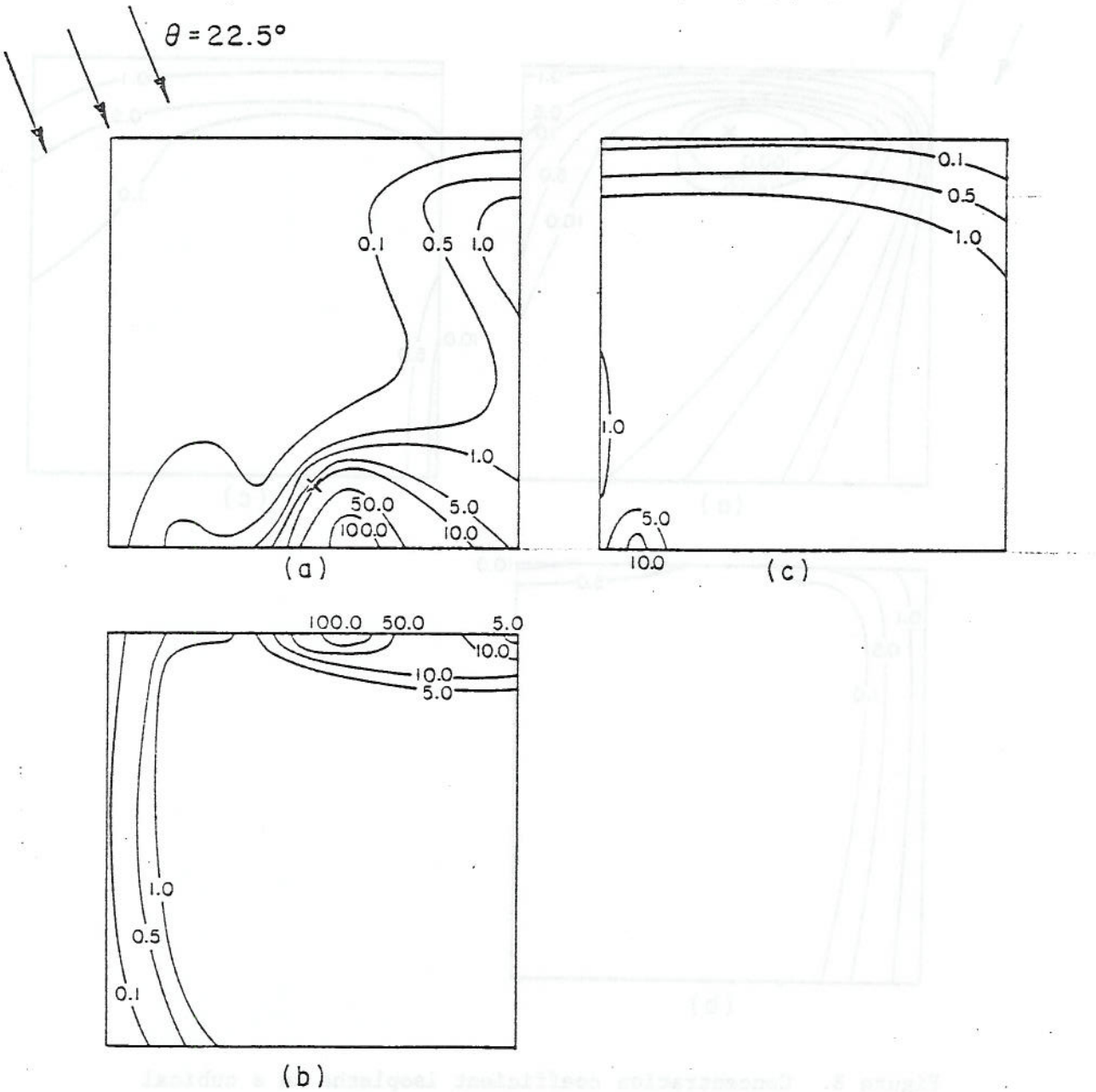

Figure 10. Concentration coefficient isopleths, K, on a cubical model building (θ = 22.5°, downwind roof vent release).

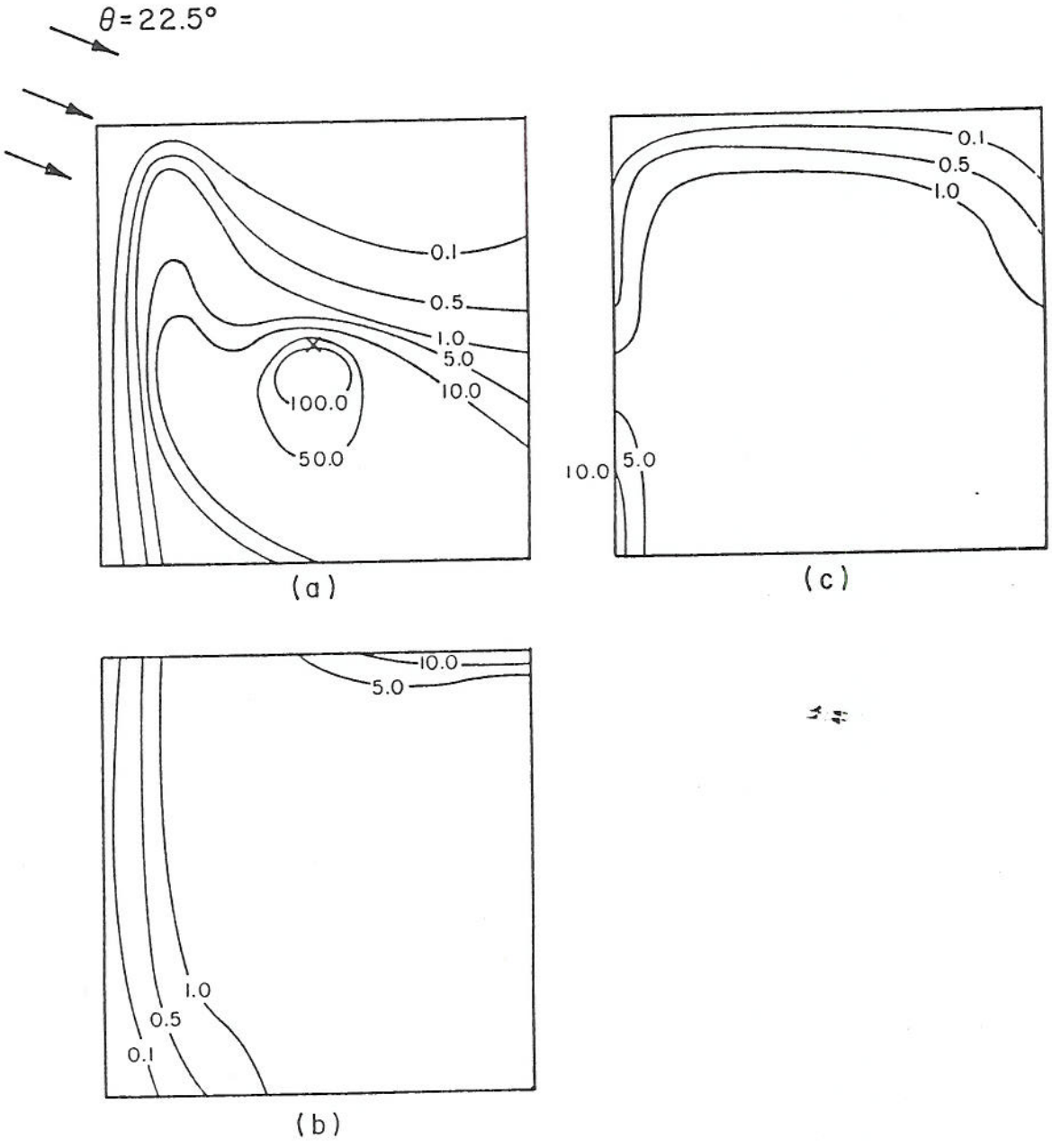

Figure 9. Concentration coefficient isopleths on a cubical model building (θ = 22.5°, central roof vent release).

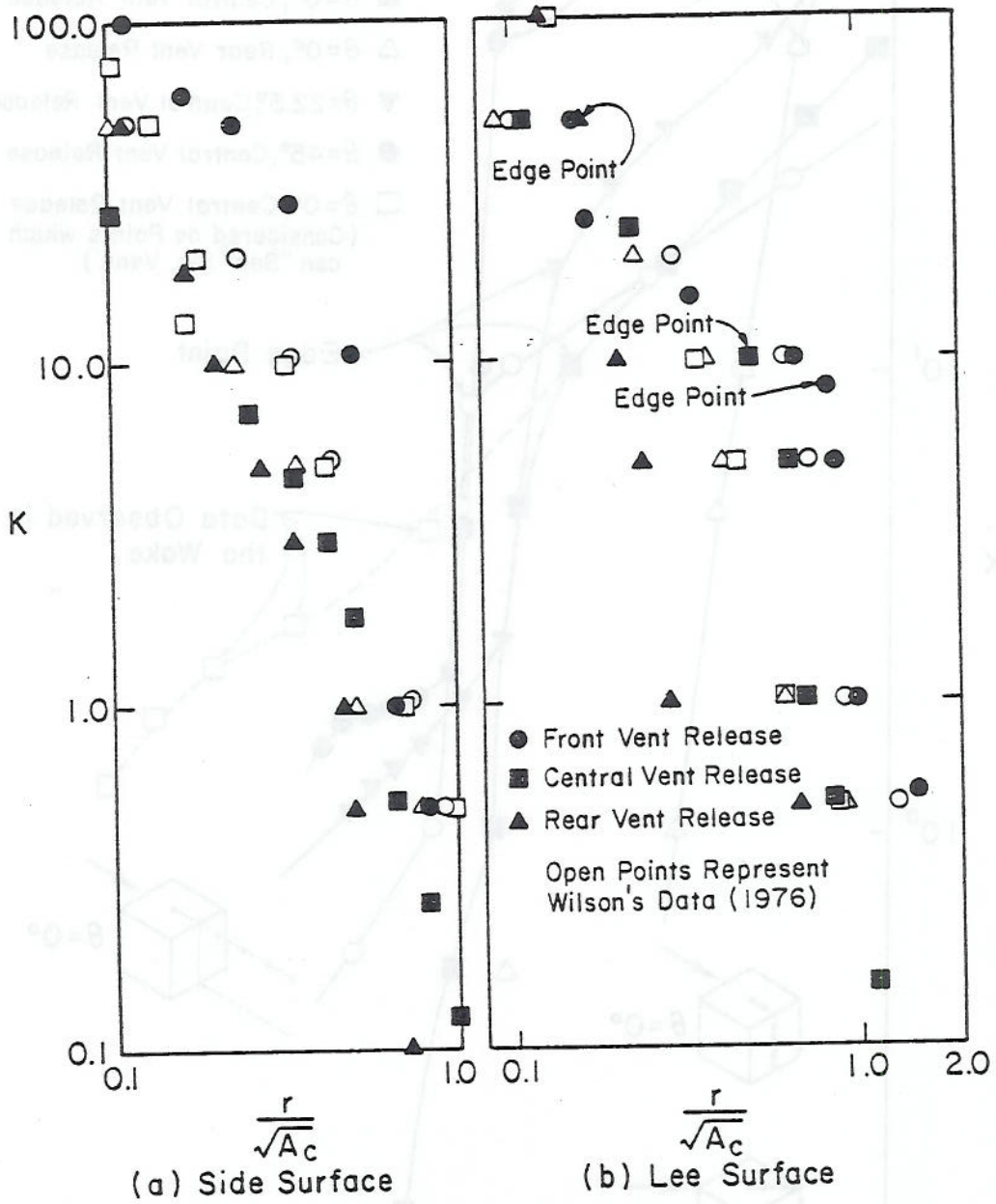

Figure 11. Surface concentration coefficients vs. string distance from the vent.

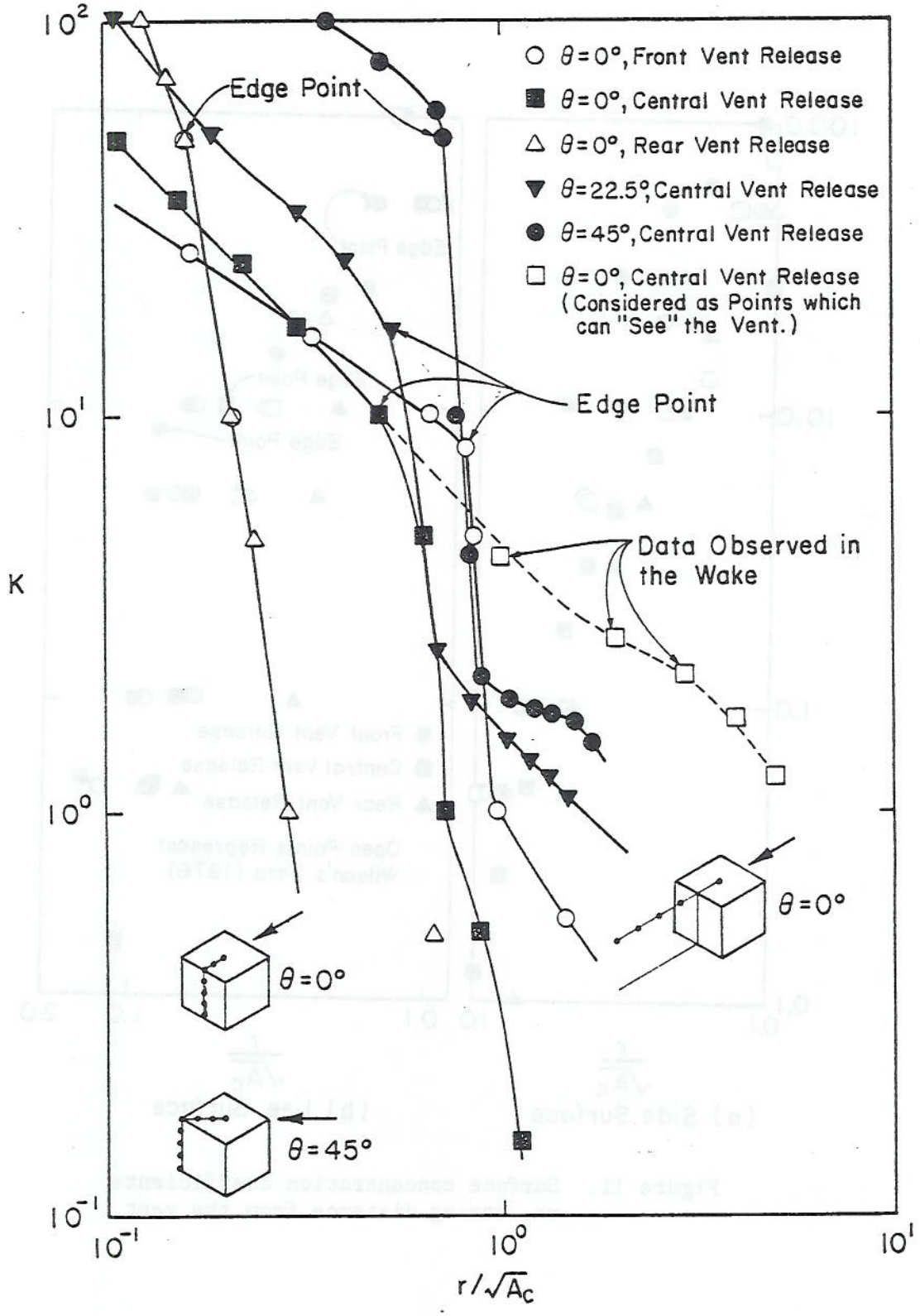

Figure 12. Concentration coefficients on the building surface along the wind direction.

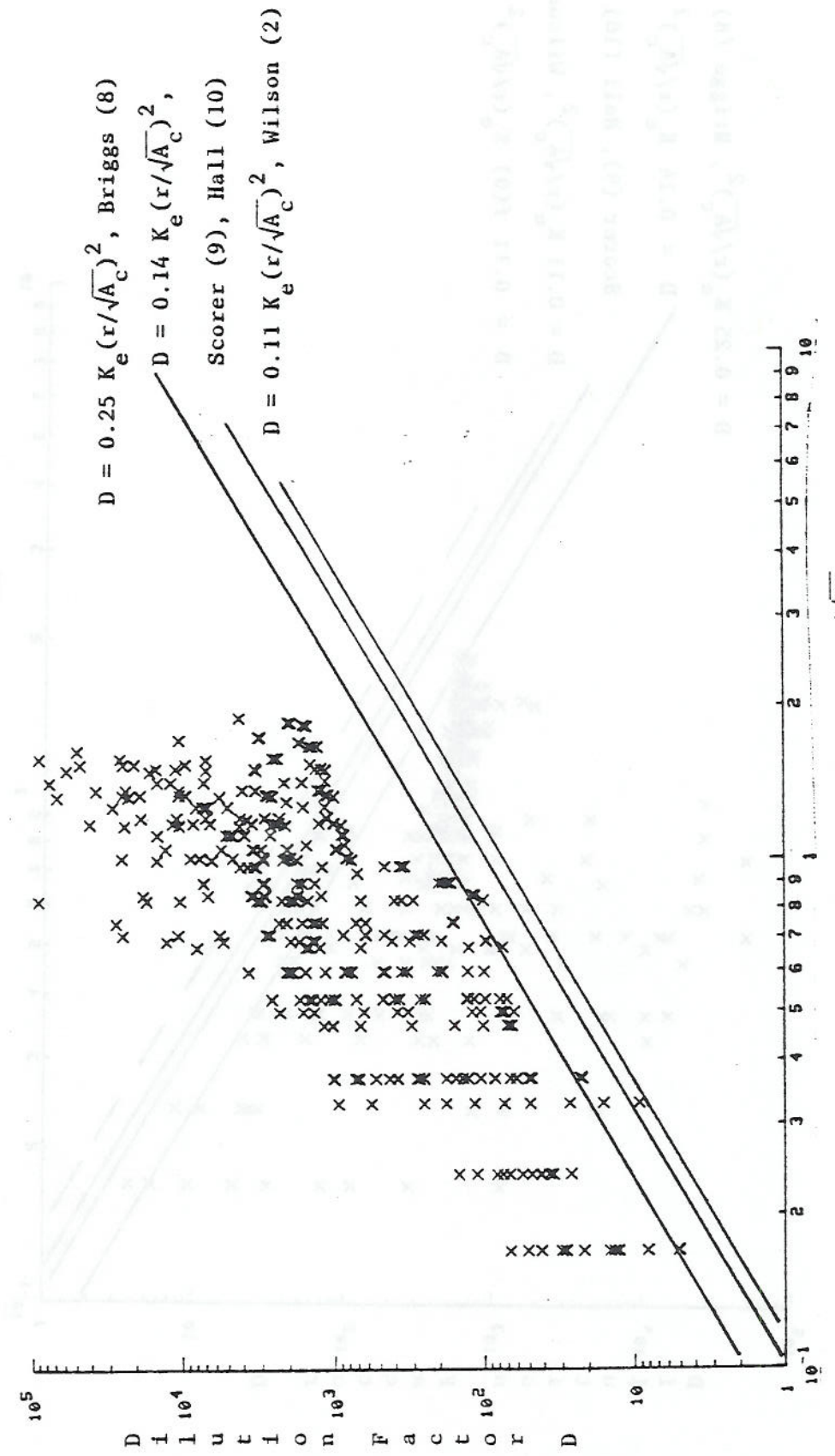

Figure 13. Dilution factors on the building for $\theta = 0°$ orientation where $K_e = 660$.

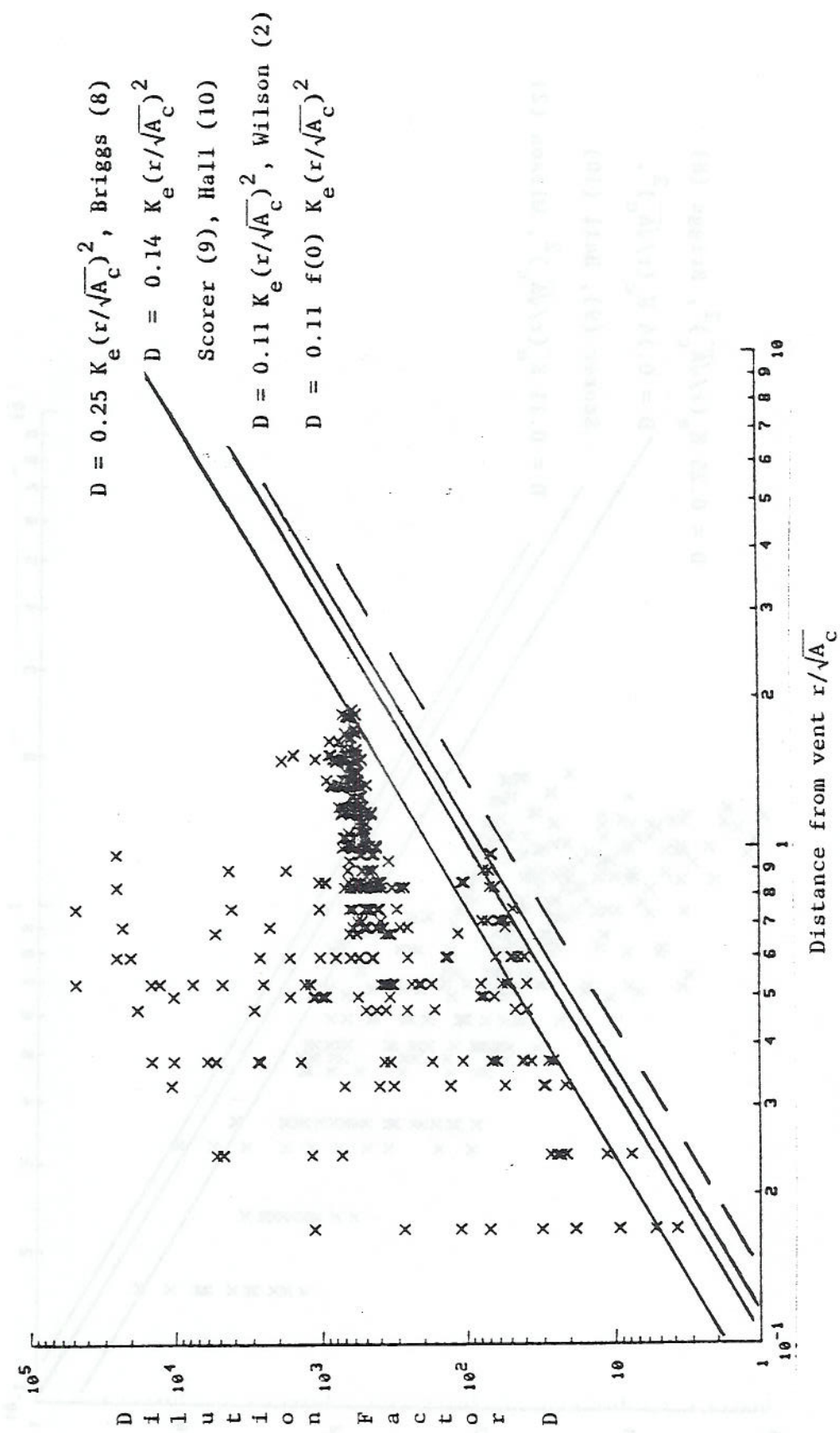

Figure 14. Dilution factors on the building for $\theta = 22.5°$ orientation where $K_e = 660$.

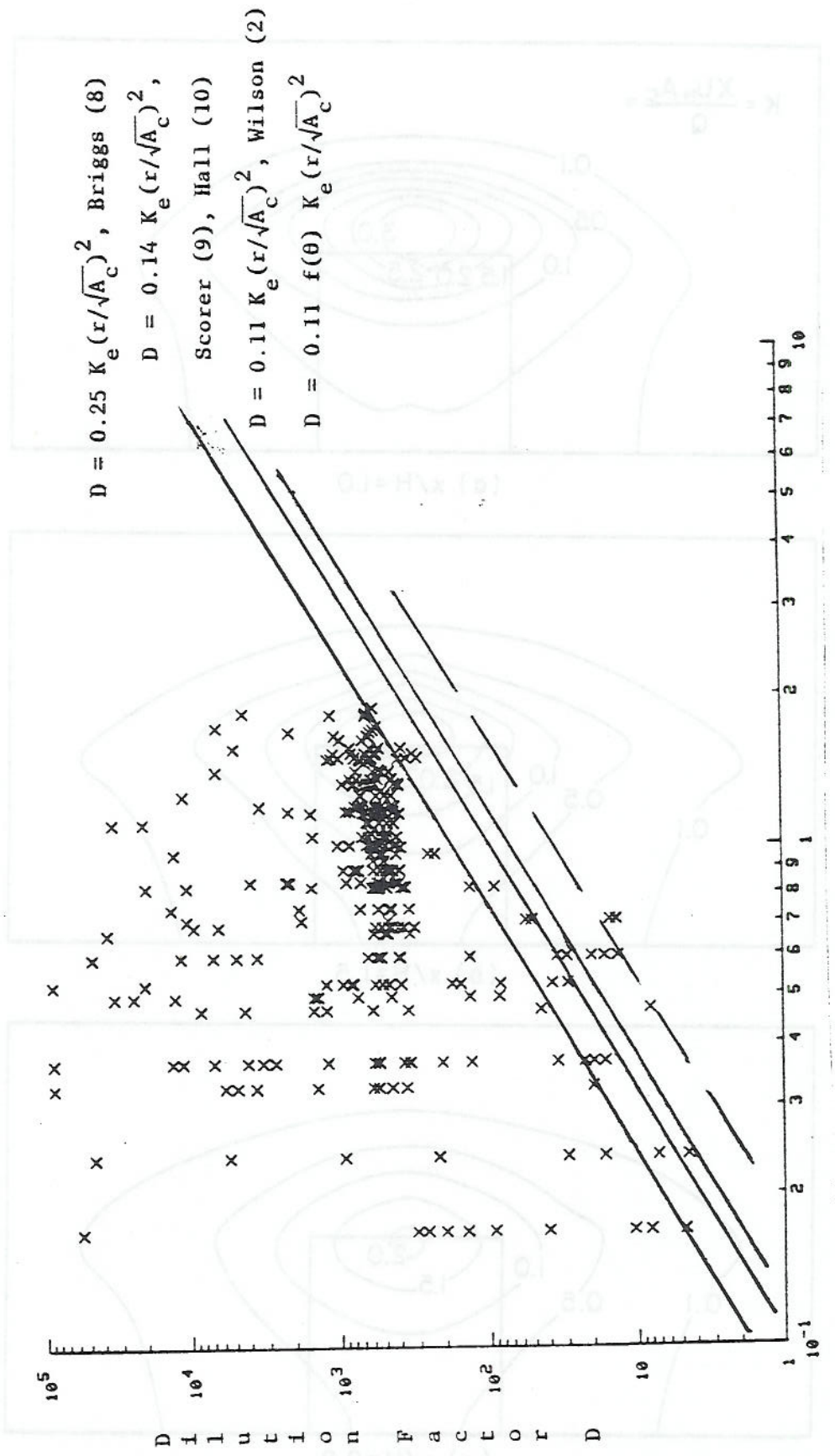

Figure 15. Dilution factors on the building for $\theta = 45°$ orientation where $K_e = 660$.

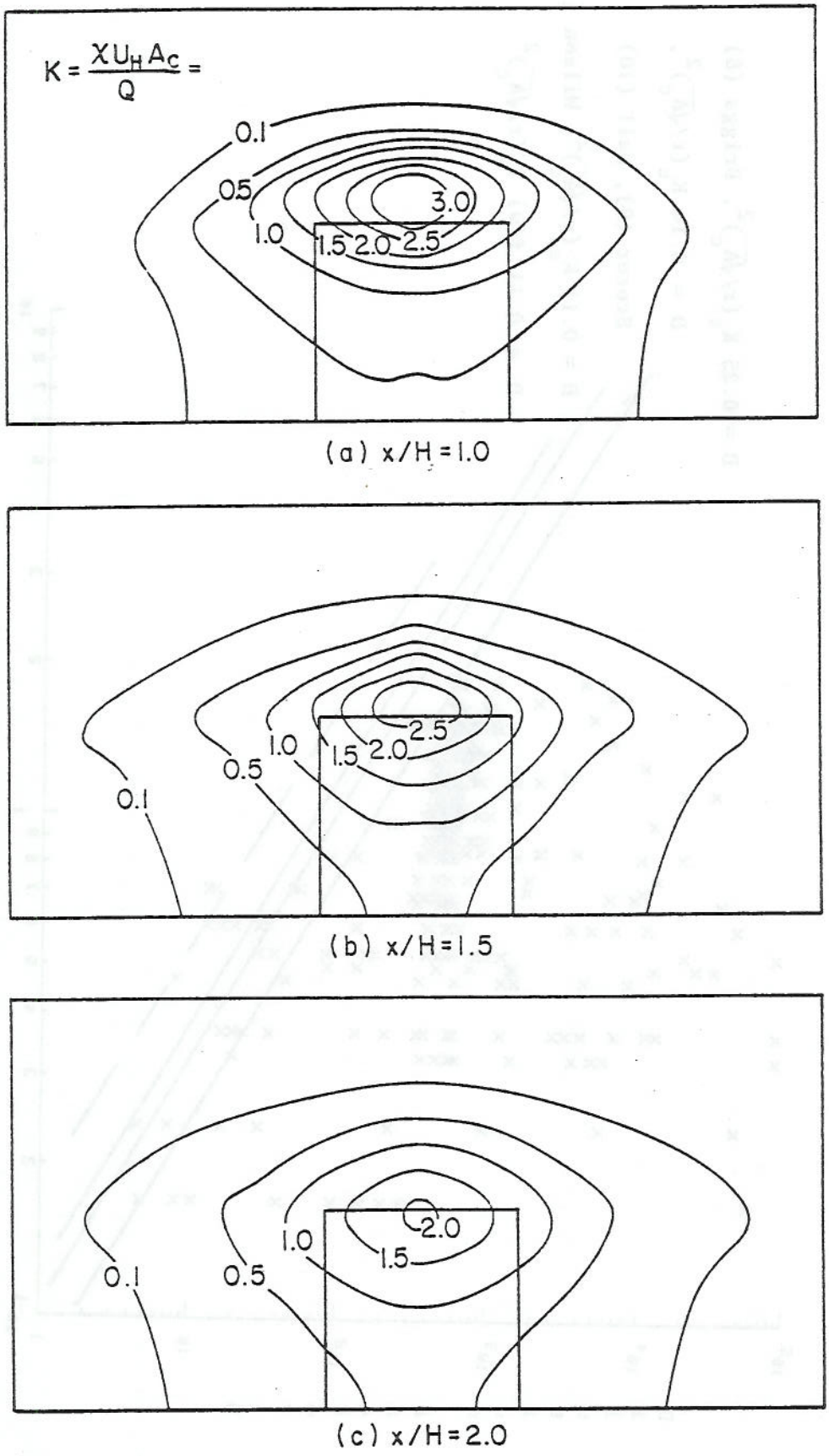

Figure 16. Concentration coefficient isopleths in the near wake region for $\theta = 0°$, central roof vent release.

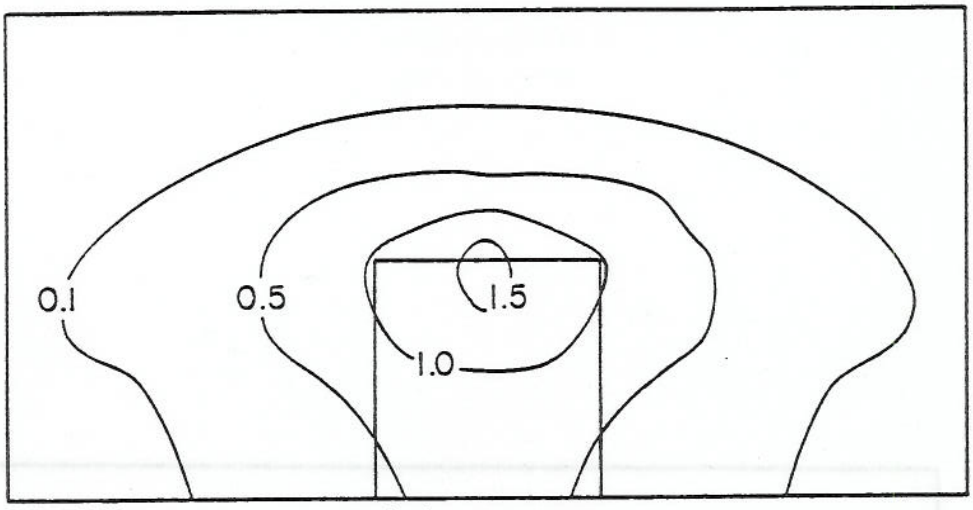

(d) x/H = 2.5

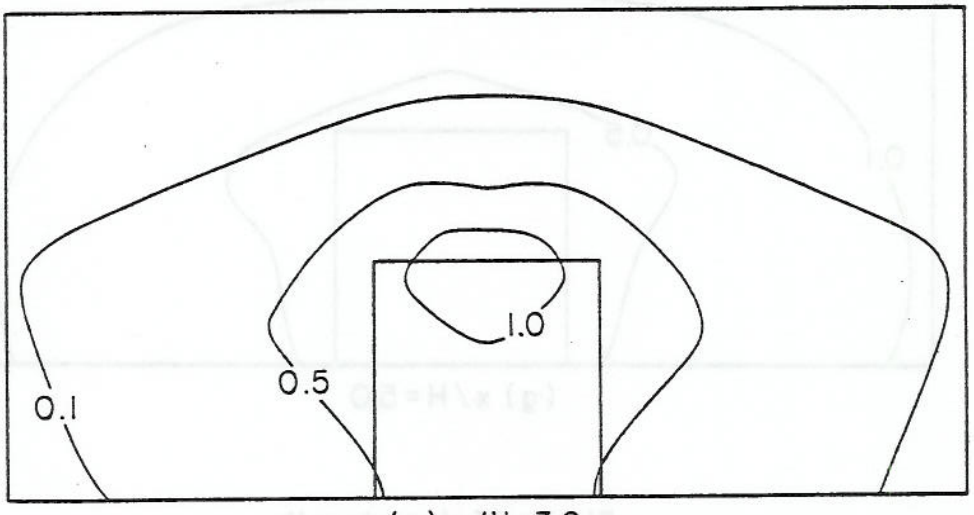

(e) x/H=3.0

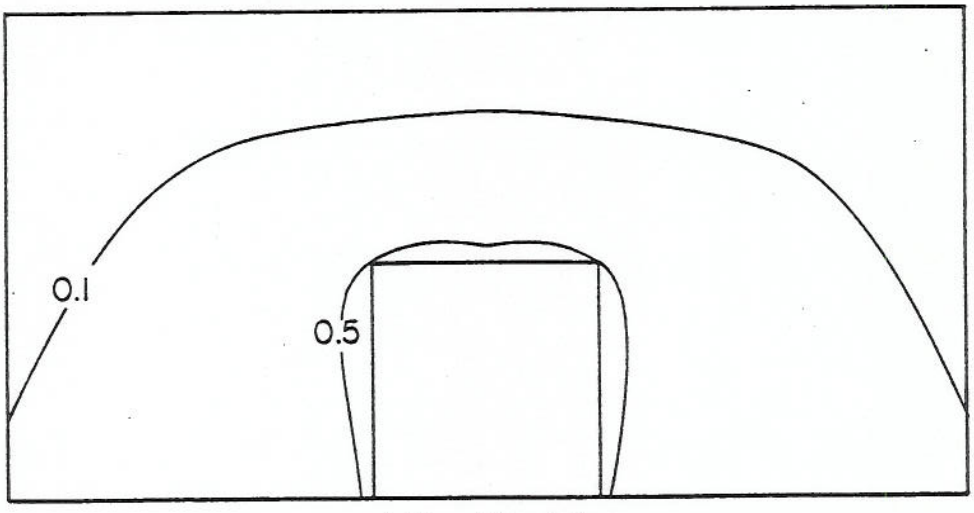

(f) x/H=4.0

Figure 16 (continued).

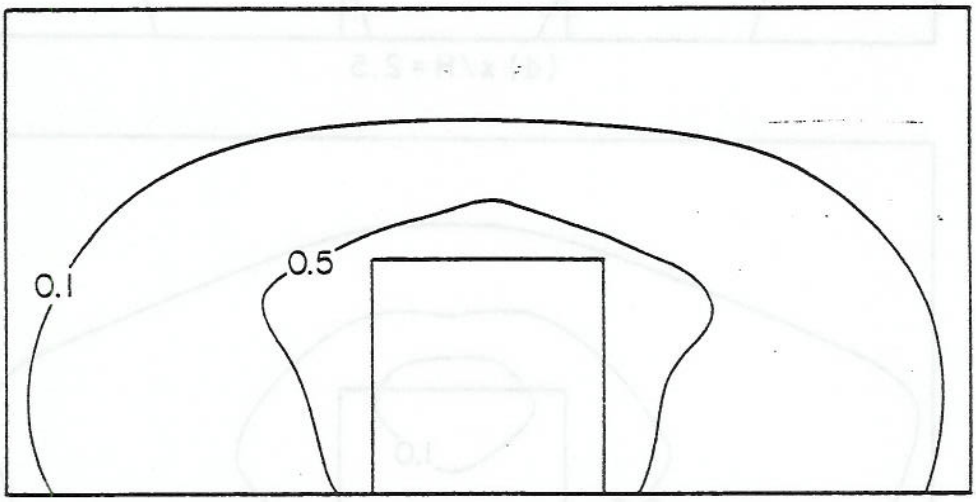

(g) x/H = 5.0

Figure 16 (continued).

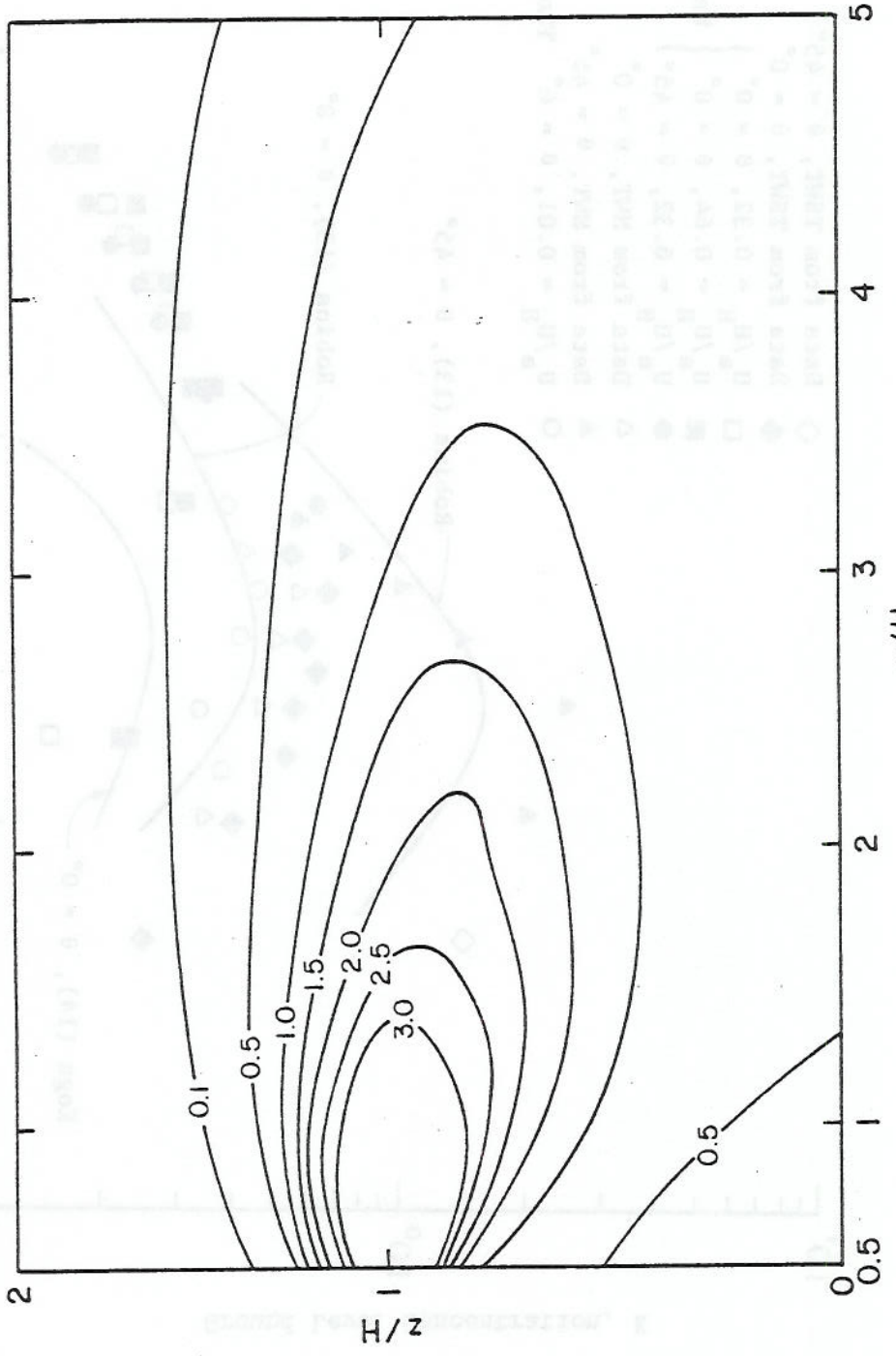

Figure 17. Longitudinal concentration coefficient distributions at Y = 0 and θ = 0° orientation, central roof vent release.

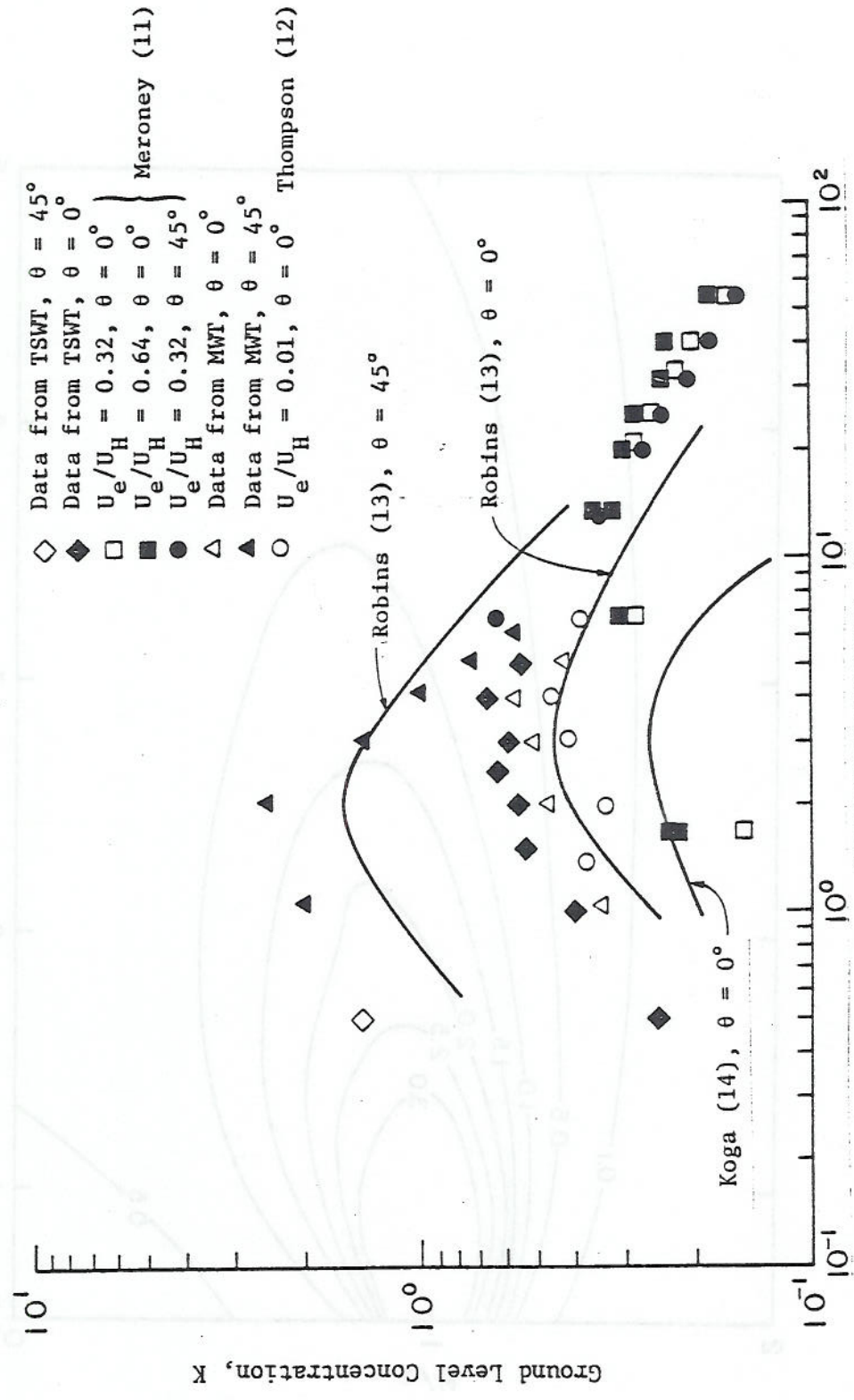

Figure 18. Maximum ground concentrations in the near wake region for θ = 0° central roof vent release. (TST: Thermally Stratified Tunnel, MWT: Meteorological Wind Tunnel.)

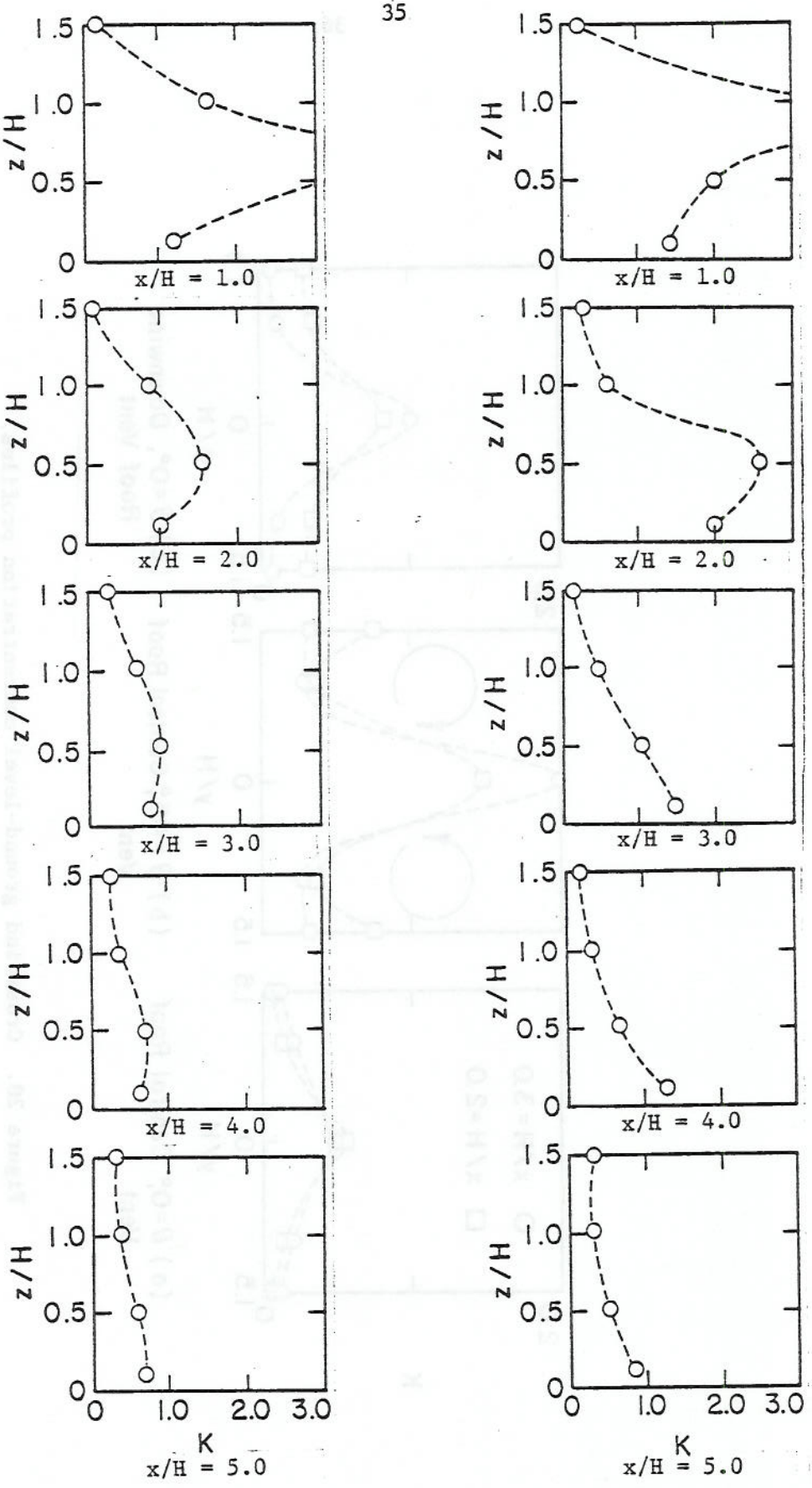

(a) Y = 0 for θ = 0°, downwind roof vent release

(b) Y = 0 for θ = 45°, central roof vent release

Figure 19. Vertical mean concentration profiles in the near wake region.

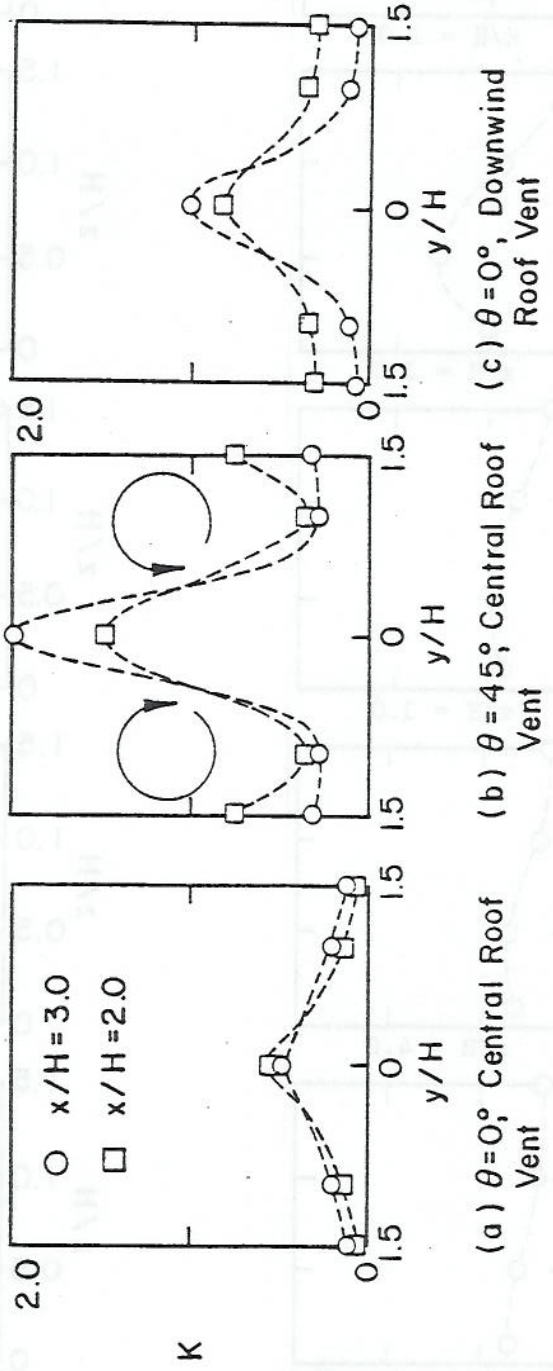

Figure 20. Crosswind ground-level concentration profiles.

LIST OF FIGURES

LIST OF FIGURES (continued)